Available online at www.sciencedirect.com
SCIENCE DIRECT®
International Journal of Mass Spectrometry 228 (2003) 933–954
International Journal of Mass Spectrometry
www.elsevier.com/locate/ijms

Structural determinants for the evaporation of intact oligomers from collisionally activated cluster ions

Da Ren[1], Michael J. Polce, Chrys Wesdemiotis*

Department of Chemistry, The University of Akron, 190 E. Buchtel Commons, Akron, OH 44325-3601, USA

Received 27 February 2003; accepted 15 April 2003

Dedicated to Professor Helmut Schwarz on the occasion of his 60th birthday and in acknowledgment of his numerous and outstanding contributions to gas phase ion chemistry and mass spectrometry.

Abstract

The dissociation mechanisms of various types of cluster ions are elucidated by direct detection and characterization of the neutral products evaporated from the cluster ions upon collisionally activated dissociation. The cluster ions investigated include proton- or sodium ion-bound oligomers of ionic and protic molecules. The experiments are complemented by quantum chemistry methods at the semiempirical PM3 level for insight on the geometries and energetics of the cluster ions and the neutral oligomers evaporated from them. The combined experimental and computational data reveal that the structure of the decomposing cluster ion determines whether complete (neutral) oligomers are eliminated from the cluster ion or whether the cluster ion "shrinks" by sequential monomer losses. An intact oligomer is eliminated only if its components already interact with each other in the cluster ion, for example, through hydrogen bonds or ion pairs (salt bridges). From the cluster ions that allow for such interligand interactions, complete oligomer and consecutive monomer evaporation are competitive, the yield of intact oligomer (dimer, trimer, etc.) loss increasing with the binding energy of oligomer in respect to the separated monomers. Ionic interactions (salt bridges) in the neutral clusters generally bring upon higher binding energies than hydrogen bonding.

Keywords: Clusters; Cluster evaporation; Neutral fragment reionization; Amino acid clusters; Salt bridges

1. Introduction

Clusters are considered as an intermediate state in the transition between the gas phase and condensed phases [1,2]. Consequently, the mechanisms, energetics and dynamics of the formation and dissociation of cluster ions, which can be studied by mass spectrometry, have been an intense area of research. These studies have aimed at a better understanding, at the molecular level, of the transformations of matter during phase changes [1–3]. Similarly, ion–molecule reactions of cluster ions have been used to probe solvent effects on the outcome and rates of chemical reactions.

A subject of particular interest has been the evaporation mechanism of proton- and metal ion-bound clusters, specifically whether their dissociation involves the sequential elimination of individual neutral molecules (monomers) or the elimination of dimers and other complete oligomers [4]. Beam experiments

* Corresponding author. Tel.: +1-330-9727699; fax: +1-330-9727370.
E-mail address: wesdemiotis@uakron.edu (C. Wesdemiotis).
[1] Present address: Waters Corporation, 34 Maple St., Milford, MA 01757, USA.

1387-3806/$ – see front matter
doi:10.1016/S1387-3806(03)00194-5

with proton-bound clusters of simple molecules, such as $(H_2O)_nH^+$ and $(NH_3)_nH^+$, have revealed that metastable cluster ions tend to lose one monomer in the microsecond time window [4]. Collisionally activated dissociation (CAD) generally increases the number of eliminated monomer molecules by promoting consecutive evaporation events [4]. An exception to this reactivity was found by Lifshitz and Feng for proton-bound formic and acetic acid clusters, $(RCOOH)_nH^+$, which also lose dimers both in the metastable time frame and upon CAD [5,6]. Dimer evaporation becomes the favored decomposition path at $n \geq 6$ with formic (R = H) [5] and $n \geq 8$ with acetic acid (R = CH_3) [6], as determined from comparison of the kinetic energy release distributions (KERDs) for monomer vs. dimer loss from metastable precursor ions and the corresponding branching ratios in metastable ion (MI) and CAD spectra [5,6]; for formic acid clusters, the one-step evaporation of an intact dimer was also confirmed by reionization of the neutral [5]. The elimination of a $(RCOOH)_2$ dimer was also observed from mixed $(RCOOH)_n(H_2O)_mH^+$ clusters past a certain critical value of $n + m$ [5,6].

Similar dissociation dynamics had been reported earlier by El-Sayed and co-workers for metastable $(CsI)_nCs^+$ ions [7,8]; the kinetic energy release distributions resulting from the loss of one and two CsI molecules were consistent with the elimination of $(CsI)_2$ dimers starting with $n = 5$. More recent experiments in our laboratory characterized directly the molecules evaporated from collisionally activated $(CsI)_nCs^+$ and $(NaI)_nNa^+$ via neutral fragment reionization mass spectrometry (N_fRMS) [9]. It was found that dimers and larger oligomers are eliminated during CAD. The largest neutral loss corresponded to the complete "solvent shell", i.e. $(CsI)_n$ or $(NaI)_n$, for $n \leq 4$ and to $(CsI)_5$ for $(CsI)_6I^+$ precursors [9].

The present study investigates the evaporation mechanism upon CAD of several types of small cluster ions composed of identical or different molecules. The investigated species include Na^+-bound dimers and trimers of sodium acetate and sodium succinate, H^+-bound trimers of cytosine, glycerol and amino acids, as well as mixed H^+-bound trimers of amino acids and sulfuric acid; a number of larger cluster ions of the same molecule (tetra- to heptamers) are also examined. The cluster ions selected for study contain monomers that can potentially interact with each other via hydrogen bonding and/or ion pair formation. The neutral dissociation products from these clusters are elucidated by N_fRMS in order to determine whether the complex constituents are evaporated individually or in the form of dimers, trimers, etc. The structures of selected trimeric cluster ions and neutral dimers are additionally evaluated by empirical and semiempirical molecular orbital (MO) calculations. The main goal of this study is to ascertain the structural determinants leading to the evaporation of whole oligomers from collisionally activated cluster ions.

2. Methods

2.1. Mass spectrometry

All experiments were performed with a modified Micromass AutoSpec tandem mass spectrometer of EBE geometry (E, electric sector; B, magnetic sector), which has been described in detail elsewhere [10]. The instrument contains two collision cells (CC-1 and CC-2) and an intermediate ion deflector in the field-free region between the magnet and the second electric sector. This configuration allows for both conventional CAD as well as N_fRMS experiments [9].

The cluster ions studied were produced by fast atom bombardment (FAB) ionization using a 12 keV Cs^+ beam as bombarding particles. The secondary ions formed upon this process were accelerated to 8.0 keV, and the desired cluster ion was mass selected by EB and subjected to CAD in CC-1. Scanning the second electric sector yielded the corresponding CAD spectrum, which shows the ionic fragments generated upon collisional activation. For assessment of the complementary neutral fragments, all ions exiting CC-1 were deflected and the remaining beam of neutral fragments was collisionally reionized in CC-2 to afford the corresponding N_fR spectrum. He and O_2 served as the CAD and reionization target gases, respectively; their

pressure was adjusted for ca. 20% main beam attenuation with each gas. Collisions of neutral species with O_2 cause collisionally induced dissociative ionization (CIDI) to cations [11–14]. In a few cases, O_2 was replaced by Xe in order to reionize to anions [15]. For spectra with an adequate signal/noise ratio, ca. 100 CAD and 300–1000 N_fR scans were summed, leading to a reproducibility in relative abundances of better than ±10% in CAD and ±20% in N_fR spectra.

The FAB matrices used were concentrated sulfuric acid for the proton-bound clusters containing H_2SO_4 and glycerol for all other cluster ions. The proper cluster constituents were mixed with the matrix to form a saturated solution and a few microliters of the final mixture were applied onto the sample holder and introduced into the vacuum system. Matrices were purchased from Fisher Scientific (Pittsburgh, PA) and the other compounds were purchased from Aldrich (Milwaukee, WI); all chemicals were used as received from the manufacturers.

2.2. Calculations

The structures of selected trimer precursor ions and neutral dimers were optimized by MO calculations. Low-energy geometries were searched by molecular mechanics/dynamics [16], using the MM2 program available in Chem3D Pro (version 4.0) [17]. The most stable conformers found were subsequently optimized fully at the semiempirical PM3 level [18] using the MOPAC algorithm included in Chem3D Pro.

3. Results and discussion

3.1. Na^+-bound sodium acetate and sodium succinate clusters

The major collision-induced fragmentations of Na^+-bound sodium acetate clusters, $(CH_3COONa)_n Na^+$ (n = 2–7), involve cleavages of one or more CH_3COONa units (cf. CAD spectra in Figs. 1 and 2). The losses of up to (n − 1) CH_3COONa molecules proceed with considerable yield. The loss of all n ligands of Na^+ also takes place in all cases albeit with markedly lower relative abundance. Are the CH_3COONa ligands eliminated consecutively or as intact oligomers (Scheme 1)? To answer this question, the N_fR spectra of $(CH_3COONa)_n Na^+$ were acquired and are displayed in Figs. 1 and 2 next to the respective CAD spectra.

The N_fR spectra contain the reionization products of all neutral fragments from CAD of $(CH_3COONa)_n Na^+$ [9]. If the CH_3COONa units are eliminated sequentially, only ions up to the m/z value of $CH_3COONa^{\bullet+}$ (m/z 82) should be observed in the N_fR spectra (Scheme 2). On the other hand, if intact $(CH_3COONa)_x$ oligomers are eliminated, the N_fR spectra should contain ions heavier than $CH_3COONa^{\bullet+}$. Collisional reionization of $(CH_3COONa)_x$ is expected to produce $(CH_3COONa)_{x-1}Na^+$ signature ions that contain *the same* number of Na atoms as the neutral cluster (Scheme 3) [9]. The $(CH_3COONa)_x^{\bullet+}$ molecular ions are unlikely to survive intact the reionizing collision, because of a low binding energy compared to the internal energy deposited upon collisional ionization at keV kinetic energies [19].

In addition to the $(CH_3COONa)_{x-1}Na^+$ signature ion, reionization of $(CH_3COONa)_x$ will also generate smaller fragment ions, viz. $(CH_3COONa)_{x-y}Na^+$ ($y \leq x$), which correspond to signature ions of smaller clusters $(CH_3COONa)_{x-y}$. Due to this overlap, N_fR spectra are most useful for the identification of the largest neutral loss, whose signature ion cannot originate but from this loss.

Upon CAD, $(CH_3COONa)_2Na^+$ dissociates chiefly by elimination of one CH_3COONa molecule (Fig. 1a). The signature ions of the latter molecule, viz. m/z 82, 43 and 23 (Scheme 2), are detected in the N_fR spectrum of Fig. 1a (m/z 82 just above noise level), confirming the presence of CH_3COONa in the beam of neutral CAD fragments generated from $(CH_3COONa)_2Na^+$. The N_fR spectrum of $(CH_3COONa)_2Na^+$ also displays a relatively abundant $(CH_3COONa)Na^+$ product at m/z 105 which, according to the arguments presented above, is characteristic of intact $(CH_3COONa)_2$ dimers. Hence, the N_fR data provide evidence that the dissociation

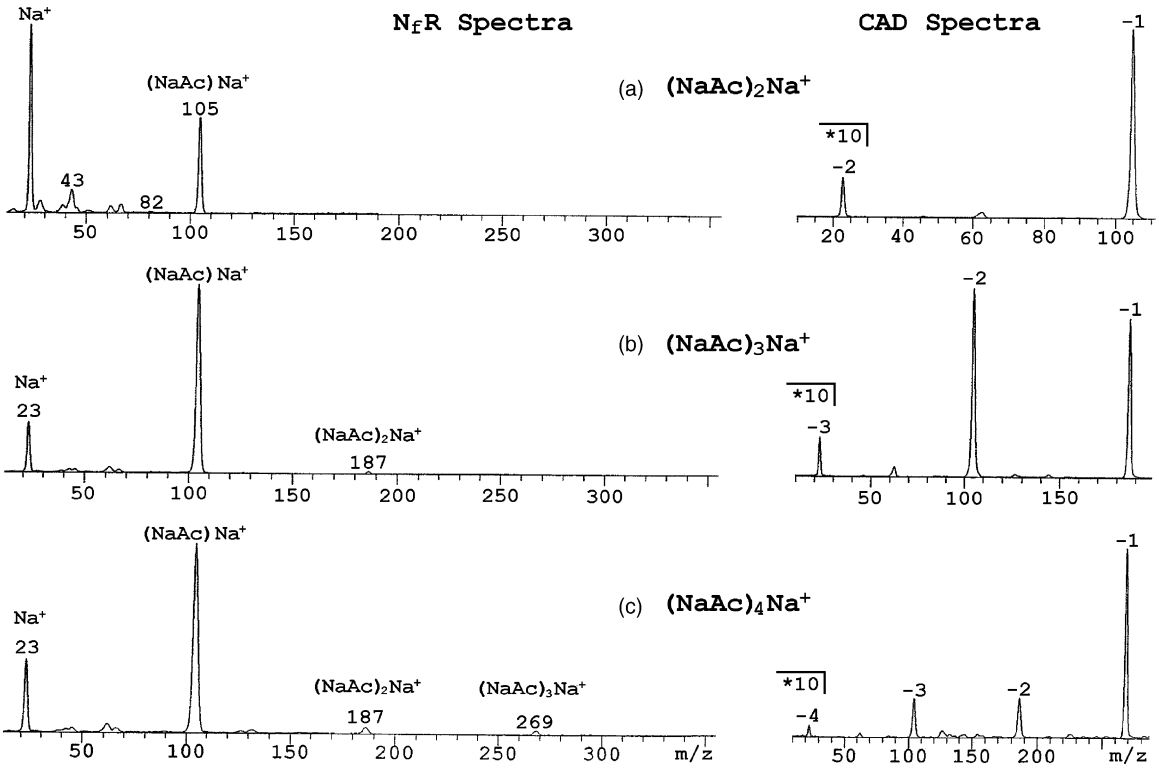

Fig. 1. CAD (right) and N_fR (left) mass spectra of Na^+-bound sodium acetate clusters, $(CH_3COONa)_nNa^+$. CH_3COONa is abbreviated as NaAc: (a) $n = 2$ (m/z 187); (b) $n = 3$ (m/z 269); (c) $n = 4$ (m/z 351). The numbers on top of CAD peaks indicate the number of NaAc units lost to form the corresponding ions. The compositions and/or m/z values of important N_fR ions are marked on top of the corresponding peaks.

$$(CH_3COONa)_nNa^+ \xrightarrow{\text{CAD}} (CH_3COONa)_{n-x}Na^+ + \begin{cases} x \cdot CH_3COONa \\ \text{or} \\ (CH_3COONa)_x \end{cases}$$

Scheme 1. Evaporation mechanisms of Na^+-bound sodium acetate clusters.

$(CH_3COONa)_2Na^+ \rightarrow Na^+$ liberates, at least in part, whole $(CH_3COONa)_2$ dimers.

Similarly, cluster ion $(CH_3COONa)_3Na^+$ shows a small, but nonetheless clearly detectable ($CH_3COONa)_2Na^+$ (m/z 187) ion in its N_fR spectrum (Fig. 1b), revealing that the CAD process $(CH_3COONa)_3Na^+ \rightarrow Na^+$ partly proceeds via cleavage of an intact $(CH_3COONa)_3$ trimer. Basepeak in the N_fR spectrum of Fig. 1b is $(CH_3COONa)Na^+$ (m/z 105); this ion may result by CH_3COONa loss from $(CH_3COONa)_2Na^+$ (m/z 187). Because of the large relative abundance of m/z 105, we reason that this ion is coproduced by reionization of $(CH_3COONa)_2$ dimers eliminated in the dissociation $(CH_3COONa)_3Na^+ \rightarrow (CH_3COONa)Na^+ +$

$$CH_3COONa \xrightarrow{\text{reionization}} CH_3COONa^{+\bullet}\ (m/z\ 82) \begin{cases} \rightarrow CH_3CO^+\ (m/z\ 43) \\ \rightarrow Na^+\ (m/z\ 23) \end{cases}$$

Scheme 2. N_fR signature ions for CH_3COONa monomer.

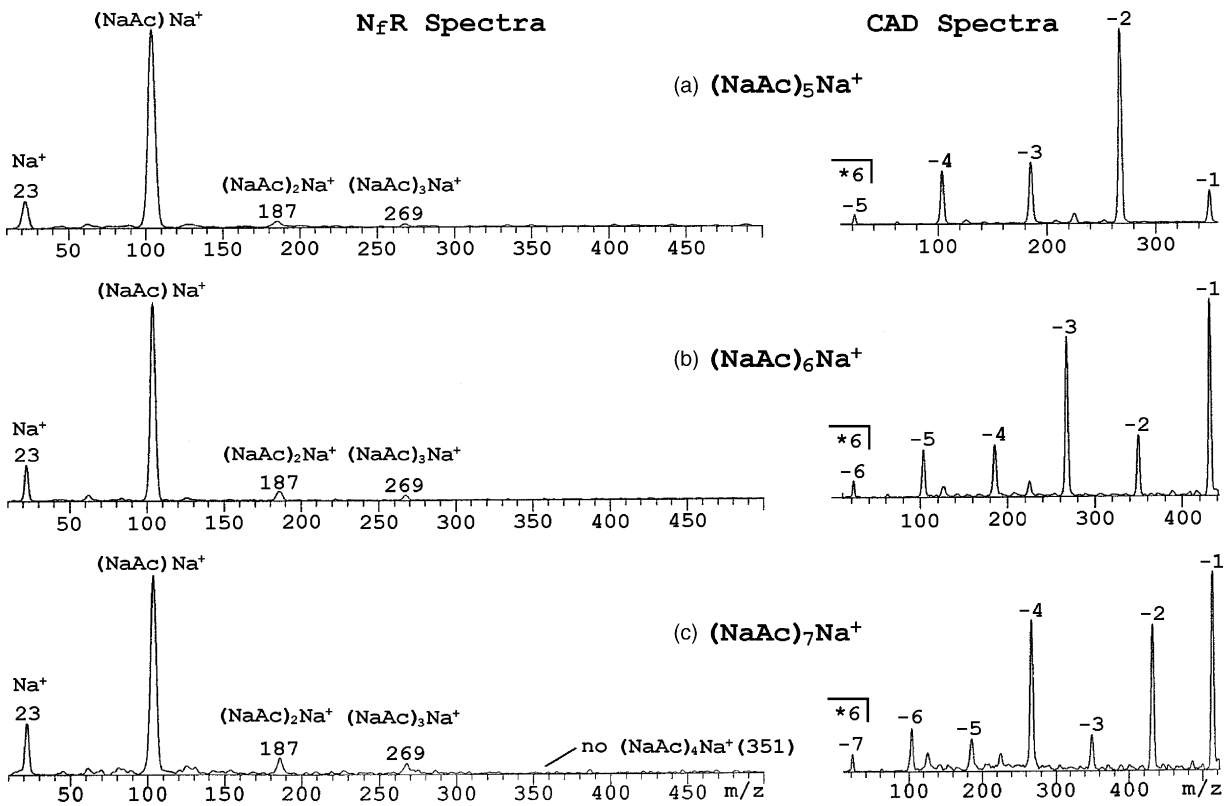

Fig. 2. CAD (right) and N_fR (left) mass spectra of Na^+-bound sodium acetate clusters, $(CH_3COONa)_nNa^+$. CH_3COONa is abbreviated as NaAc: (a) $n = 5$ (m/z 433); (b) $n = 6$ (m/z 515); (c) $n = 7$ (m/z 597). The numbers on top of CAD peaks indicate the number of NaAc units lost to form the corresponding ions. The compositions and/or m/z values of important N_fR ions are marked on top of the corresponding peaks.

$(CH_3COONa)_2$ (elimination of two CH_3COONa units is the major CAD channel of $(CH_3COONa)_3Na^+$).

An analogous situation is encountered for $(CH_3COONa)_4Na^+$ cluster ions. Their N_fR spectrum (Fig. 1c) contains $(CH_3COONa)_3Na^+$ (m/z 269), i.e., the signature ion of $(CH_3COONa)_4$ tetramers. This result provides evidence that Na^+ can be formed from $(CH_3COONa)_4Na^+$ in one step, by elimination of a whole $(CH_3COONa)_4$ tetramer. A sizable $(CH_3COONa)_2Na^+$ (m/z 187) ion is also present in the N_fR spectrum of Fig. 1c, and the basepeak again is $(CH_3COONa)Na^+$ (m/z 105). The two

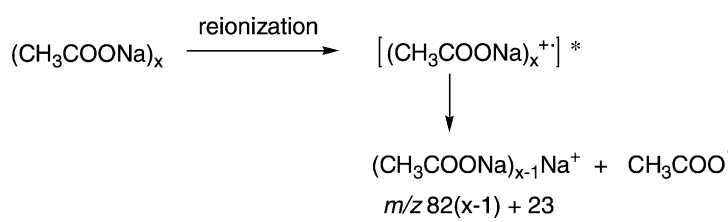

Scheme 3. N_fR signature ion for $(CH_3COONa)_x$ oligomer.

latter N_fR products most probably originate from reionization of intact $(CH_3COONa)_3$ trimers and $(CH_3COONa)_2$ dimers, respectively, cleaved directly from the $(CH_3COONa)_4Na^+$ precursor ion upon CAD; of course, these ions may also arise from consecutive fragmentation of the signature ion of the largest neutral loss, viz. $(CH_3COONa)_4$.

Overall, the N_fR data of Fig. 1 present strong evidence that $(CH_3COONa)_nNa^+$ cluster ions with $n = 2-4$ can lose their entire "solvent shell", i.e., all ligands, in one piece during CAD. A different behavior is found for $(CH_3COONa)_nNa^+$ clusters with $n = 5-7$. Now, the largest neutral loss detected above noise level in the corresponding N_fR spectra (Fig. 2) is $(CH_3COONa)_4$ (its signature ion is $(CH_3COONa)_3Na^+$ at *m/z* 269). The losses of overall 5, 6, and 7 CH_3COONa units are, however, detected in the CAD spectra (Fig. 2). Evidently, these reactions involve consecutive eliminations of two (or more) neutral molecules, for example, $(CH_3COONa)_7Na^+ \rightarrow Na^+ + (CH_3COONa)_4 + (CH_3COONa)_3$, presumably because the elimination of the smaller neutral clusters is more readily feasible from the structures of the larger cluster ions.

In principle, the neutral species evaporated can also be characterized by reionization into negative

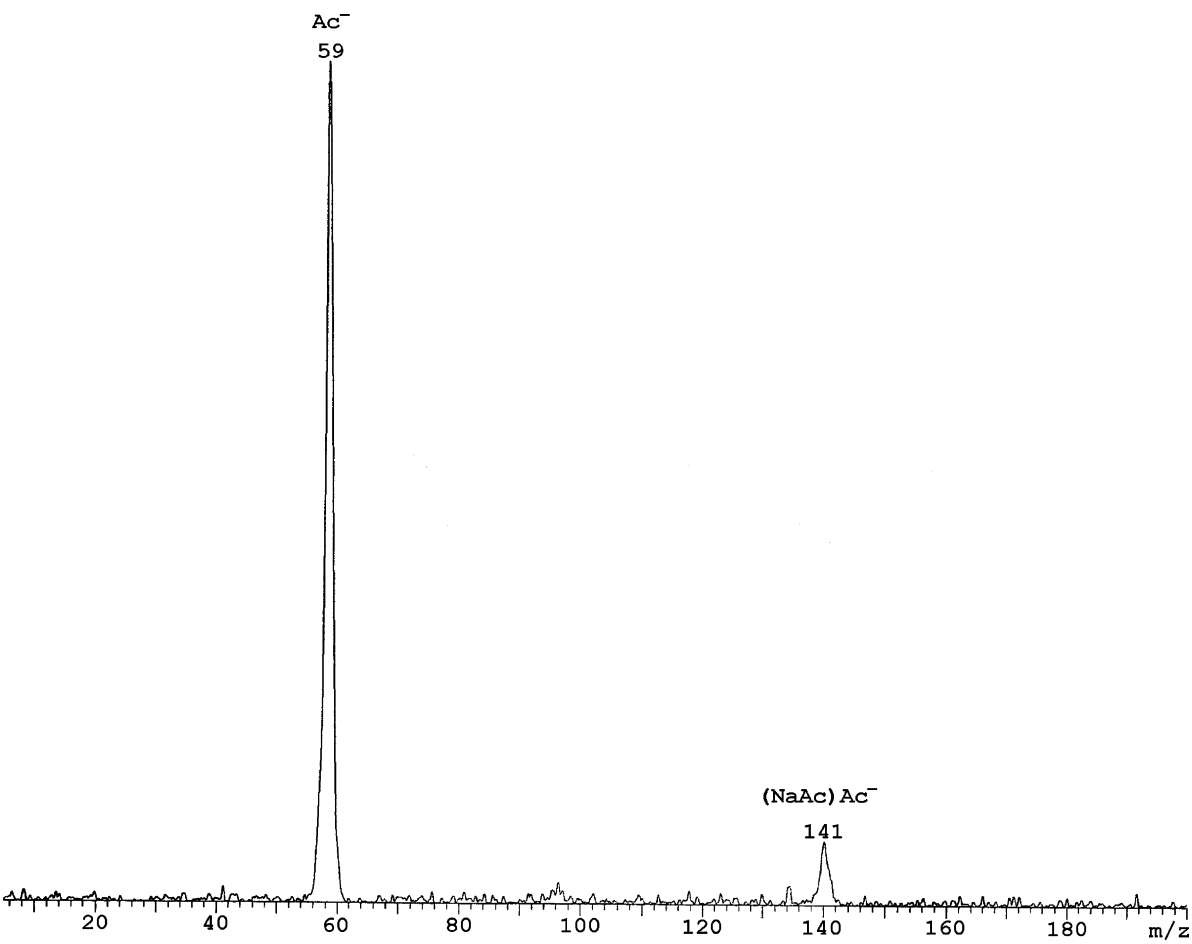

Fig. 3. N_fR^- spectrum of $(CH_3COONa)_2Na^+$ (*m/z* 187). CH_3COO^- and CH_3COONa are abbreviated as Ac^- and NaAc, respectively. The compositions and *m/z* values of the N_fR^- products are indicated on top of the corresponding peaks.

ions (N_fR^-). Such a process is, however, associated with a substantially lower yield than the alternative reionization to positive ions [9]. For this reason, a useable N_fR^- spectrum could only be obtained from $(CH_3COONa)_2Na^+$ clusters, which are formed with the highest intensity upon FAB ionization. This spectrum is shown in Fig. 3 and includes two clearly discernable products, CH_3COO^- (*m/z* 59) and $(CH_3COONa)CH_3COO^-$ (*m/z* 141). The latter anion contains two acetate units and, thus, diagnoses that the $(CH_3COONa)_2Na^+$ precursor ion must have lost an intact $(CH_3COONa)_2$ dimer upon CAD, in agreement with the N_fR data from reionization to cations (Fig. 1a).

Sodium ion-bound sodium succinate clusters with 2–4 monomer units, $(NaOOCCH_2CH_2COONa)_nNa^+$ (n = 2–4), were also studied. For brevity, these species will be named $(Na_2Suc)_nNa^+$. These clusters mainly lose 1 to n Na_2Suc (sodium succinate) units, in analogy to the sodium acetate clusters discussed. In the corresponding N_fR spectra, ions heavier than the ionized Na_2Suc monomer are observed, indicating that complete Na_2Suc oligomers are eliminated during the collision-induced evaporation process. Such evaporation behavior is identical with that found for $(CH_3COONa)_{2–4}Na^+$ clusters (vide supra).

3.2. Proton-bound clusters of glycerol and cytosine

Proton-bound clusters of glycerol, $(C_3H_8O_3)_nH^+$, and cytosine, $(C_4H_5N_3O)_nH^+$, composed of n = 3–5 monomers are readily and abundantly formed in the FAB ion source. Upon CAD, these cluster ions primarily lose one or more (up to $n-1$) monomer units, as shown in Figs. 4 and 5 (top right part) for the protonated pentamers. The question raised before for the Na^+-bound clusters can also be asked in this case: are the molecules eliminated sequentially or as large oligomers? The answer is found in the corresponding N_fR spectra (Figs. 4 and 5, left part).

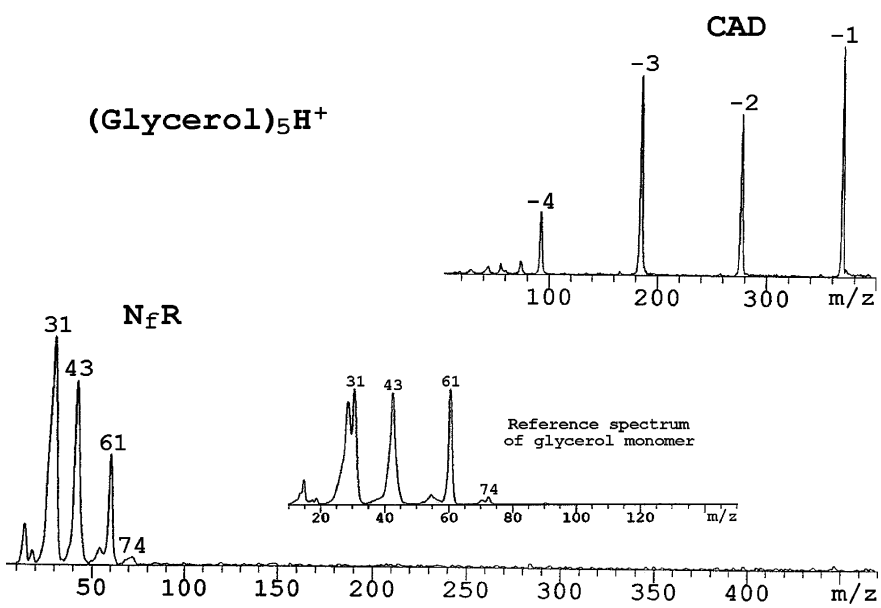

Fig. 4. CAD (top right) and N_fR (bottom left) mass spectra of $(glycerol)_5H^+$ (*m/z* 461). The numbers on top of CAD peaks indicate the number of glycerol units lost to form the corresponding ions. The *m/z* values of important N_fR ions are marked on top of the corresponding peaks. The N_fR spectra of $(glycerol)_3H^+$ and $(glycerol)_4H^+$ are similar to the spectrum of $(glycerol)_5H^+$. The middle inset shows the N_fR spectrum of $(glycerol)_2H^+$, which represents a reference spectrum of glycerol monomer because the proton-bound dimer only loses one glycerol molecule upon CAD (Scheme 4).

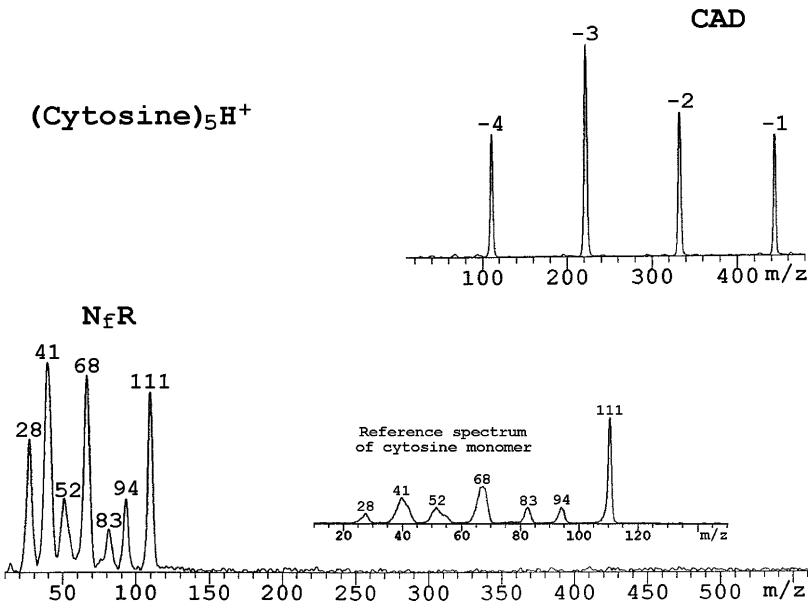

Fig. 5. CAD (top right) and N_fR (bottom left) mass spectra of $(cytosine)_5H^+$ (*m*/*z* 556). The numbers on top of CAD peaks indicate the number of cytosine units lost to form the corresponding ions. The *m*/*z* values of important N_fR ions are marked on top of the corresponding peaks. The N_fR spectra of $(cytosine)_3H^+$ and $(cytosine)_4H^+$ are similar to the spectrum of $(cytosine)_5H^+$. The middle inset shows the N_fR spectrum of $(cytosine)_2H^+$, which represents a reference spectrum of cytosine monomer because the proton-bound dimer only loses one cytosine molecule upon CAD.

The N_fR spectra of $(glycerol)_nH^+$ ($n = 3$–5) are practically indistinguishable, containing abundant *m*/*z* 31, 43, and 61 ions as well as a detectable *m*/*z* 74 ion (Fig. 4). The masses of these N_fR products lie below that of glycerol (92 u). A reference collisional ionization spectrum of glycerol molecules was obtained by using H^+-bound dimers, whose CAD releases only one $C_3H_8O_3$ unit. This spectrum is shown as an inset in Fig. 4 and its products are accounted for in Scheme 4. Collisional ionization is a hard ionization method, compared to electron impact [19]; further, ionized alkanols and glycols have very low dissociation

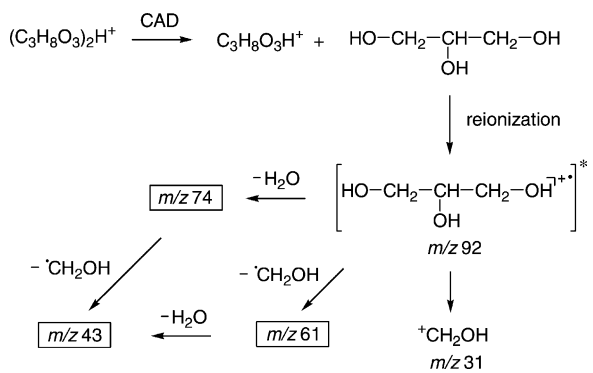

Scheme 4. Collisional ionization products of glycerol molecules, formed via CAD of $(glycerol)_2H^+$.

thresholds [20,21]. It is therefore not surprising that no glycerol molecular ion (no *m/z* 92) is observed in the reference spectrum; however, the spectrum includes several fragment ions that are diagnostic of the glycerol connectivity, such as *m/z* 74, 61, 43, and 31 (Scheme 4).

The reference spectrum of glycerol monomer is strikingly similar with the N_fR spectra of $(glycerol)_nH^+$ (n = 3–5) (cf. Fig. 4, bottom left side). Based on this fact, it is concluded that the proton-bound glycerol clusters studied dissociate via consecutive cleavages of monomer units. If intact dimers or larger oligomers had been evaporated, an N_fR signature ion above the *m/z* value of glycerol should have been observed, such as *m/z* 93 (protonated glycerol), which is a particularly stable ion [21,22].

A completely analogous evaporation reactivity is found for $(cytosine)_nH^+$ (n = 3–5) clusters. Their N_fR spectra (Fig. 5) contain ions only up to *m/z* 111, which is the mass-to-charge ratio of ionized cytosine. All N_fR ions observed are present in the reference reionization spectrum of cytosine ($C_4H_5N_3O$), which is depicted as an inset in Fig. 5. In contrast to glycerol, cytosine gives rise to a sizable $M^{\bullet+}$ upon collisional ionization, as it also does upon electron impact [23,24]. The similarity of the N_fR spectra of $(cytosine)_nH^+$ (n = 3–5) with the collisional ionization spectrum of cytosine molecule attests that the proton-bound cytosine clusters investigated undergo sequential monomer losses during CAD.

Neutral cytosine dimers have been observed in supersonic beams and must therefore be bound species [25]. Bonding interactions should also exist between glycerol molecules, which are capable of forming intermolecular hydrogen bonds. The fact that the losses of $(glycerol)_2$, $(cytosine)_2$ or larger oligomers do not take place from evaporating proton-bound clusters with up to five glycerol or cytosine units consequently means that the monomers in these cluster ions cannot interact efficiently with each other so that they are eliminated in one piece [5,6].

Alternatively, it is conceivable that oligomers are detached from $(glycerol)_nH^+$ or $(cytosine)_nH^+$ but yield no detectable signature ions in the reionization step. This scenario is unlikely; Feng and Lifshitz detected $(CH_3COOH)H^+$ signature ions in the reionization spectrum of $(CH_3COOH)_2$ dimers, which are bound via hydrogen bonds [5], similar to $(glycerol)_2$ and $(cytosine)_2$. Moreover, evidence will be presented below that other hydrogen-bonded neutral clusters indeed yield upon reionization diagnostic ions that confirm their evaporation (from larger proton-bound clusters).

3.3. Proton-bound trimers of amino acids and sulfuric acid

Sulfuric acid binds easily with amino acids to form cluster ions under FAB ionization conditions. Proton-bound trimers composed of one sulfuric acid and two amino acid (AA) units, $H_2SO_4(AA)_2H^+$, are particularly abundant. The evaporation behavior of such cluster ions with AA = aspartic acid (Asp), histidine (His), lysine (Lys), arginine (Arg) and betaine (Bet) has been studied; the selected amino acids carry acidic (Asp), basic (His, Lys) or zwitterionic (Arg, Bet) substituents. The CAD spectra of these clusters have very similar dissociation patterns (Figs. 6–8, right part). All cluster ions undergo elimination of H_2SO_4 and $H_2SO_4 + AA$. The $H_2SO_4 + AA$ units could be cleaved in one piece, as the dimer $H_2SO_4{\bullet\bullet\bullet}AA$, or consecutively (Scheme 5). The N_fR spectra (Figs. 6–8, left part) provide evidence that both these pathways take place.

The loss of H_2SO_4 from the collisionally activated $H_2SO_4(AA)_2H^+$ cluster ions is affirmed by the N_fR spectra, in which signature ions of sulfuric acid (see inset of Fig. 6) are detected, either as distinct peaks or as shoulders of more abundant N_fR products resulting from other losses. A common, important characteristic in the N_fR spectra is the presence of AAH^+ ions. The

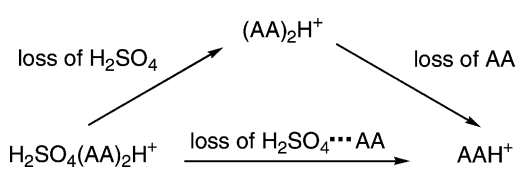

Scheme 5. Evaporation pathways of $H_2SO_4(AA)_2H^+$ cluster ions.

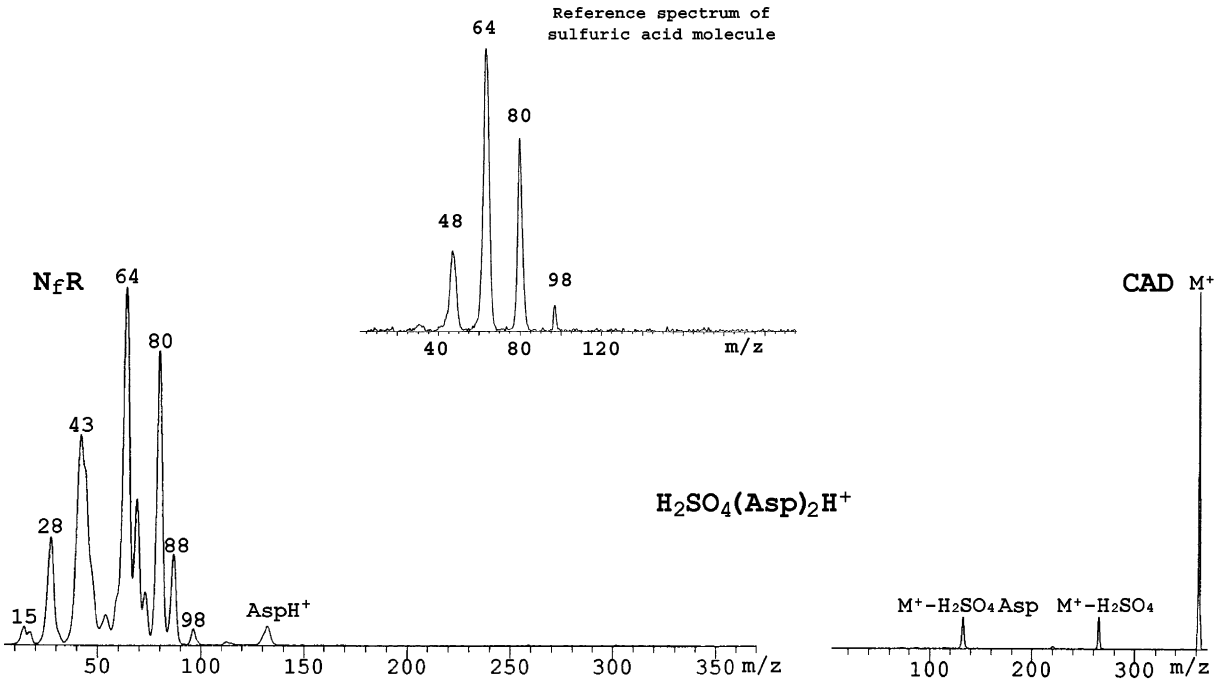

Fig. 6. CAD (right) and N_fR (left) mass spectra of H^+-bound trimer $H_2SO_4(Asp)_2H^+$ (*m/z* 365). The inset shows the N_fR spectrum of $(H_2SO_4)_3H^+$, which is used as reference spectrum for H_2SO_4 molecules; the corresponding proton-bound dimer, $(H_2SO_4)_2H^+$, also undergoes SO_3 loss and, thus, provides a less suitable reference spectrum.

appearance of such products, whose mass lies above those of AA and H_2SO_4, confirms the elimination of complete H_2SO_4●●●AA clusters from collisionally activated $H_2SO_4(AA)_2H^+$ (Scheme 5).

Sequential eliminations of H_2SO_4 and AA would yield the same fragment ion generated directly via the evaporation of H_2SO_4●●●AA (Scheme 5). Previous studies from our group have shown that the most prominent signature ions produced upon the collisional reionization of amino acids are the corresponding immonium ions and, with side-chain functionalized AA, fragment ions from the side chains [26]. The presence of AA molecules among the neutral fragments released from collisionally excited $H_2SO_4(AA)_2H^+$ clusters is indicated by the following signature ions: for Asp, *m/z* 88 (immonium ion) and 70 (Fig. 6); for His, *m/z* 110 (immonium ion) and 82 (Fig. 7a); for Lys, *m/z* 129, 101 (immonium ion) and 84 (Fig. 7b); for Arg, *m/z* 129 (immonium ion), 112, 87 and 70 (Fig. 8a); and for Bet, *m/z* 101, 73 and 58 (Fig. 8b).

Overall, the N_fR data point out that $H_2SO_4(AA)_2H^+$ cluster ions evaporate H_2SO_4 plus AA both in one piece as well as sequentially (Scheme 5). A quantitative analysis of the two pathways is impossible from the N_fR data, as the relative abundances of N_fR signature ions depend on several unknown or uncontrollable variables, such as the reionization cross-section of the respective neutral fragment and transmission/collection efficiencies [9].

It is evident from the CAD spectra of Figs. 6–8 that the stepwise evaporation of amino acid and sulfuric acid molecules commences with the elimination of H_2SO_4, which is followed by the elimination of AA (there is barely any amino acid loss directly from $H_2SO_4(AA)_2H^+$). It is also noticed that the relative abundance of AAH^+ in the N_fR spectra decreases in the order $H_2SO_4(Arg)_2H^+ \geq H_2SO_4(Bet)_2H^+ \gg$

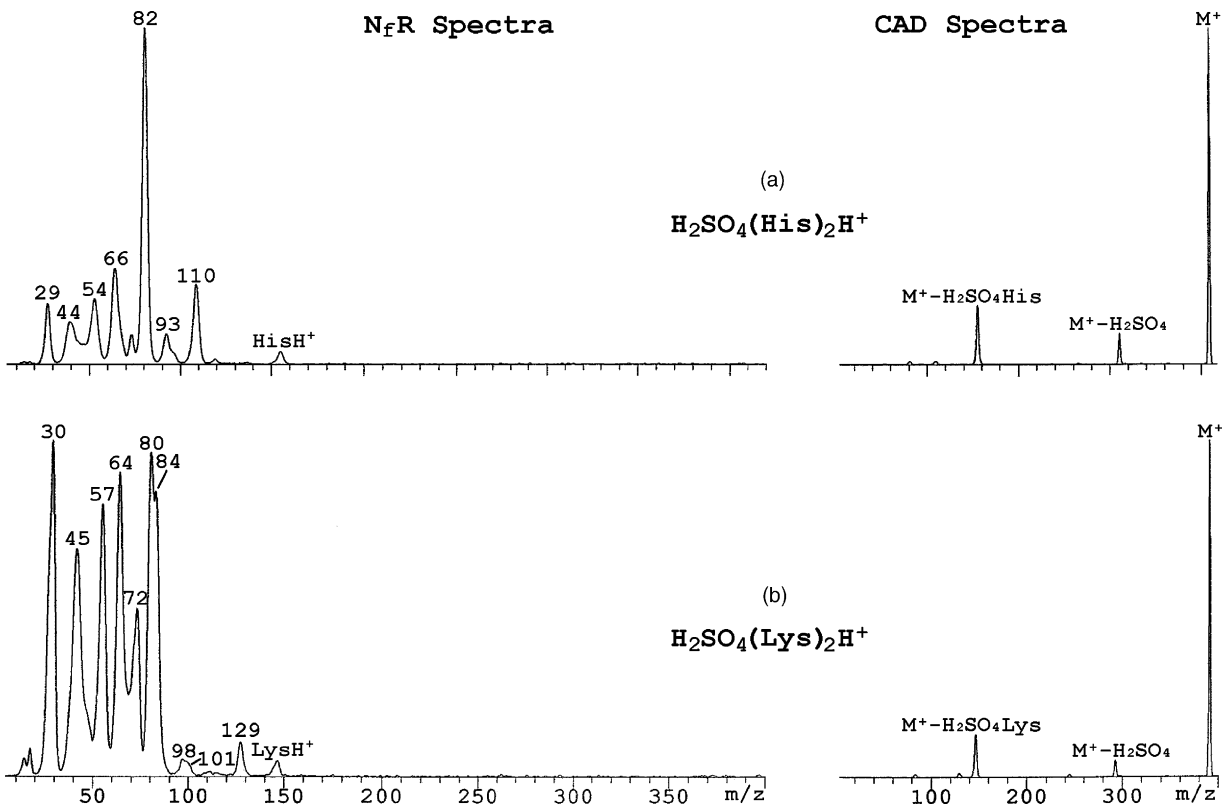

Fig. 7. CAD (right) and N_fR (left) mass spectra of H^+-bound trimers: (a) $H_2SO_4(His)_2H^+$ (*m/z* 409); and (b) $H_2SO_4(Lys)_2H^+$ (*m/z* 391).

$H_2SO_4(Lys)_2H^+ \approx H_2SO_4(His)_2H^+ \approx H_2SO_4(Asp)_2H^+$. Since the AAH^+ ion diagnoses the evaporation of intact H_2SO_4●●●AA clusters, the observed trend suggests that the proportion of H_2SO_4●●●AA loss vs. the sequential elimination of $H_2SO_4 + AA$ is substantially larger from cluster ions containing Arg and Bet than from cluster ions containing other amino acids.

The binding interaction in the H_2SO_4●●●AA clusters could involve a hydrogen bond or an ion pair (salt bridge [27,28]). In either case, the strength of the interaction depends on the gas phase acidity of the H-donor and gas phase basicity of the H-acceptor. Relevant thermochemical data are listed in Table 1 [22,29,30] and show that sulfuric acid is significantly more acidic than the AA molecules investigated, while AA are the more basic species. Hence, H_2SO_4 is the

Table 1
Proton transfer energetics of H_2SO_4 and AA (kJ/mol)[a]

Molecule	ΔH°_{acid} [b]	ΔG°_{acid} [b]	PA[c]	GB[d]
H_2SO_4	1282	1251	699	667
Asp			909	875
His	1385[e]	1356[e]	988	950
Lys	1412[e]	1383[e]	996	951
Bet			1003[f]	974[f]
Arg	1389[e]	1360[e]	1051	1007

[a] All values from Ref. [22] unless noted otherwise.
[b] ΔH° and ΔG° change of reaction $M \rightarrow [M - H]^- + H^+$ ($M = H_2SO_4$ or AA).
[c] Proton affinity; ΔH° change of reaction $MH^+ \rightarrow M + H^+$ ($M = H_2SO_4$ or AA).
[d] Gas phase basicity; ΔG° change of reaction $MH^+ \rightarrow M+H^+$ ($M = H_2SO_4$ or AA).
[e] Ref. [29].
[f] Ref. [30].

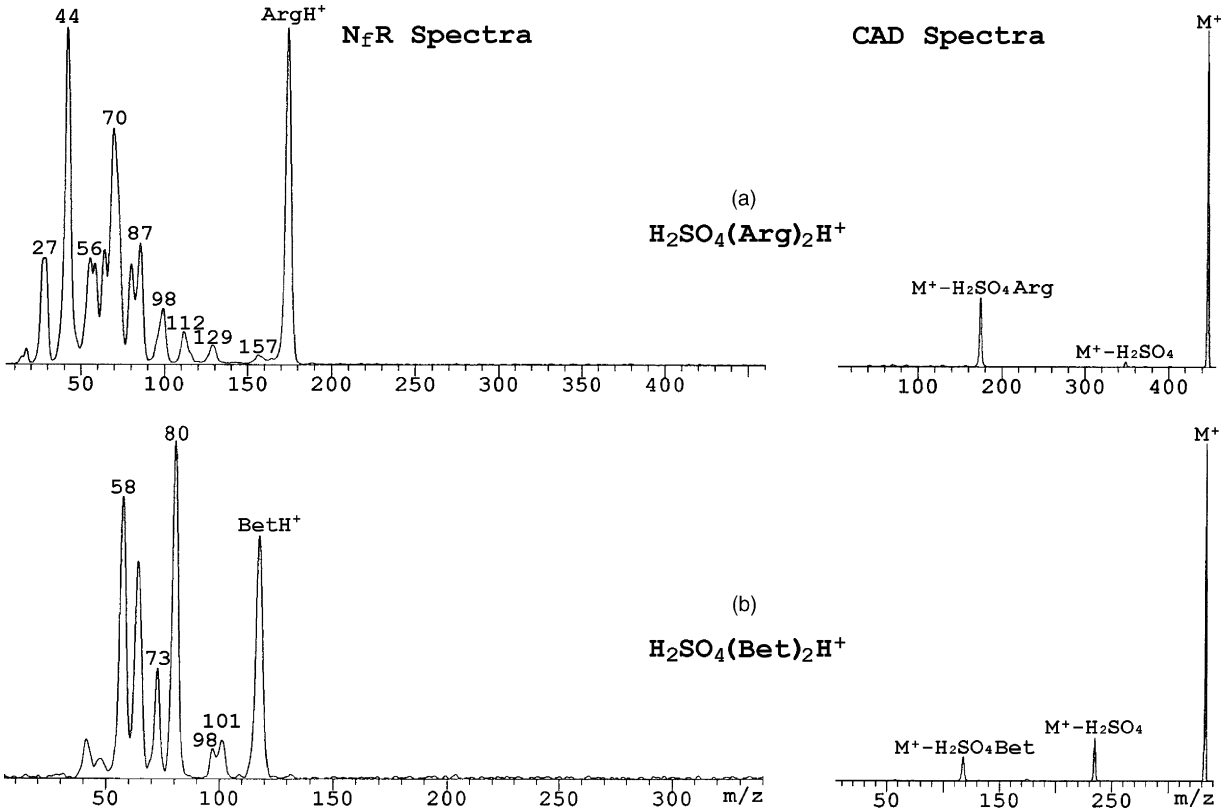

Fig. 8. CAD (right) and N_fR (left) mass spectra of H^+-bound trimers: (a) $H_2SO_4(Arg)_2H^+$ (*m*/*z* 447); and (b) $H_2SO_4(Bet)_2H^+$ (*m*/*z* 333).

acid (H-donor) and AA the base (H-acceptor) in the H_2SO_4•••AA clusters. The strongest H_2SO_4•••AA interaction is expected with the most basic amino acids Bet and Arg. The particularly high thermodynamic stability of H_2SO_4•••Bet and H_2SO_4•••Arg provides a plausible rationale for the larger extent observed for the evaporation of intact H_2SO_4•••AA clusters from precursor ions carrying Bet and Arg (vide supra).

3.4. Proton-bound trimers of arginine and betaine

The neutral fragments liberated from collisionally activated proton-bound trimers of arginine $(Arg)_3H^+$ and betaine $(Bet)_3H^+$ were also investigated. The CAD spectra of these $(AA)_3H^+$ clusters (Fig. 9, right) contain only two major fragment ions, stemming from the losses of one and two AA units. The loss of two AA units proceeds, at least in part, in one step through the elimination of whole AA•••AA dimers, because the corresponding N_fR spectra (Fig. 9, left) include ions that are higher in mass than monomeric Arg (174 u) or Bet (117 u). Specifically, the signature ion observed for Arg•••Arg is $ArgH^+$ (*m*/*z* 175; Fig. 9a, left). Similarly, Bet•••Bet produces $BetH^+$ (*m*/*z* 118) upon collisional reionization (Fig. 9b, left). The latter dimer also forms an ion of *m*/*z* 174, which nominally arises from the incipient reionized $[Bet•••Bet]^{•+}$ by loss of a 60-u neutral (e.g., acetic acid, methyl formate or CO_2 and CH_4); the mechanism of this process, which is unique to Bet•••Bet, is difficult to discern.

It is noticed that the abundances of AAH^+ (AA = Arg, Bet) in the N_fR spectra of $(AA)_3H^+$ (Fig. 9) are lower than the abundances of these ions in the N_fR spectra of $H_2SO_4(AA)_2H^+$ (Fig. 8). This difference is ascribed to the lower proportion of one-step elimination of AA•••AA from $(AA)_3H^+$, compared

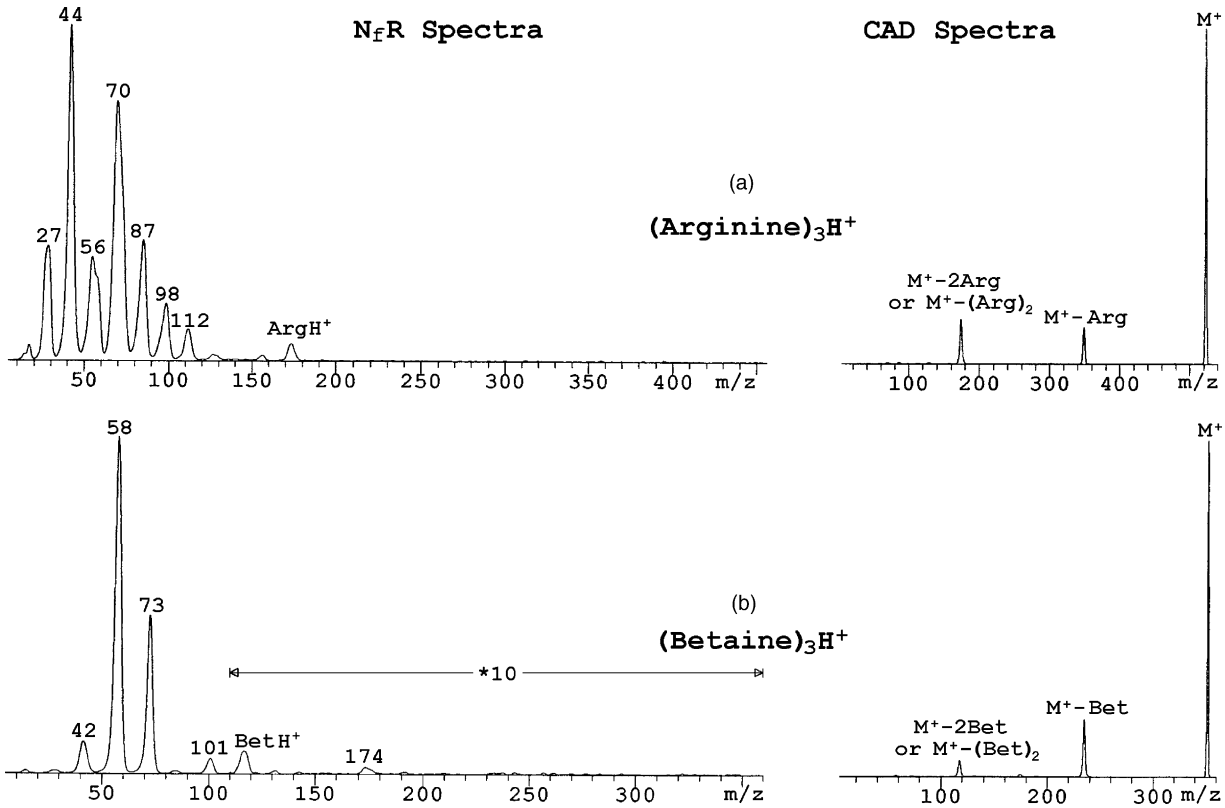

Fig. 9. CAD (right) and N_fR (left) mass spectra of H^+-bound trimers of (a) arginine, $(Arg)_3H^+$ (*m/z* 523); and (b) betaine, $(Bet)_3H^+$ (*m/z* 352).

to the one-step elimination of H_2SO_4●●●AA from $H_2SO_4(AA)_2H^+$. This supposition is supported by the abundance ratio of the two major fragments in the CAD spectra of Figs. 8 and 9. Specifically, the abundance of AAH^+ (loss of $H_2SO_4 + AA$ or $AA + AA$ in one step or sequentially) relative to that of $(AA)_2H^+$ (loss of H_2SO_4 or AA) is consistently lower in the CAD spectra of $(AA)_3H^+$ (Fig. 9) than in the CAD spectra of $H_2SO_4(AA)_2H^+$ (Fig. 8), in agreement with a lower extent of intact neutral cluster evaporation from the $(AA)_3H^+$ precursor ions.

The evaporation behavior of proton-bound trimers of glycine, histidine, aspartic acid, and lysine has also been studied. Only the elimination of monomers is observed from these cluster ions.

Recent computational studies have shown that the Arg zwitterion (designated here as $^+Arg^-$) lies slightly higher in energy than canonical Arg, the corresponding energy difference being 11–12 kJ/mol [31,32]. In contrast, the most stable form of the Arg dimer contains both arginines in the zwitterionic state ($^+Arg^-$●●●$^+Arg^-$). This dimer has a head-to-tail geometry, in which the guanidinium groups interact with the carboxylate groups through cation/anion attractive forces and hydrogen bonds; $^+Arg^-$●●●$^+Arg^-$ is predicted to lie 42 kJ/mol lower in energy than the most stable nonionic dimer [32]. Other quantum chemistry studies have found that the proton-bound dimer of Arg, viz. $(Arg)_2H^+$, contains an ion–zwitterion in its most stable structure [33]; it is reasonable to assume that such salt bridges are also present in ion $(Arg)_3H^+$ [34]. Thus, the elimination of intact dimers from $(Arg)_3H^+$ could be promoted by the fact that $^+Arg^-$●●●$^+Arg^-$ is particularly stable and that

zwitterionic arrangements are already present in the $(Arg)_3H^+$ precursor ions. Betaine-containing cluster ions show a similar reactivity, as this amino acid is naturally zwitterionic and has no stable free acid tautomer. On the other hand, the absence of detectable AA•••AA dimers among the neutral fragments released from proton-bound trimers of other amino acids could be the result of these $(AA)_3H^+$ cluster ions carrying canonical AA units, which do not develop the strong interligand (i.e., AA/AA) interactions needed for the evaporation of intact AA•••AA clusters.

3.5. Calculated structures of sodium acetate clusters

Semiempirical calculations at the PM3 level were performed on $(CH_3COONa)_2$, $(CH_3COONa)_3$ and $(CH_3COONa)_3Na^+$ in order to appraise the structure and binding energy of the neutral dimer and trimer and the structure of the sodium ion-bound trimer from which these oligomers (and the monomer) are evaporated. The energy-minimized structures of the neutral and ionic clusters are shown in Fig. 10. The binding energies of the neutral dimer and trimer are considerable (128 and 223 kJ/mol, respectively, cf. Table 2), owing to the ionic interactions possible between the associated monomers. It is interesting to note that the optimized geometries of $(CH_3COONa)_2$ and $(CH_3COONa)_3$ have cyclic structures, in which the Na^+ cations are coordinated by two acetate ligands. In $(CH_3COONa)_3Na^+$, the extra Na^+ ion is located in the center of the $(CH_3COONa)_3$ ring, interacting with six O sites to achieve a favorable multidentate coordination. Dimer $(CH_3COONa)_2$ can be formed with minimal rearrangement from $(CH_3COONa)_3Na^+$ by elimination of one $(CH_3COONa)Na^+$ segment from the periphery. Similarly, detachment of the central Na^+ from the Na^+-bound trimer readily yields $(CH_3COONa)_3$. All these factors justify the experimentally observed occurrence of intact $(CH_3COONa)_2$ dimer and $(CH_3COONa)_3$ trimer (the complete ligand shell) evaporation from collisionally activated $(CH_3COONa)_3Na^+$ (see Section 3.1 and Fig. 1).

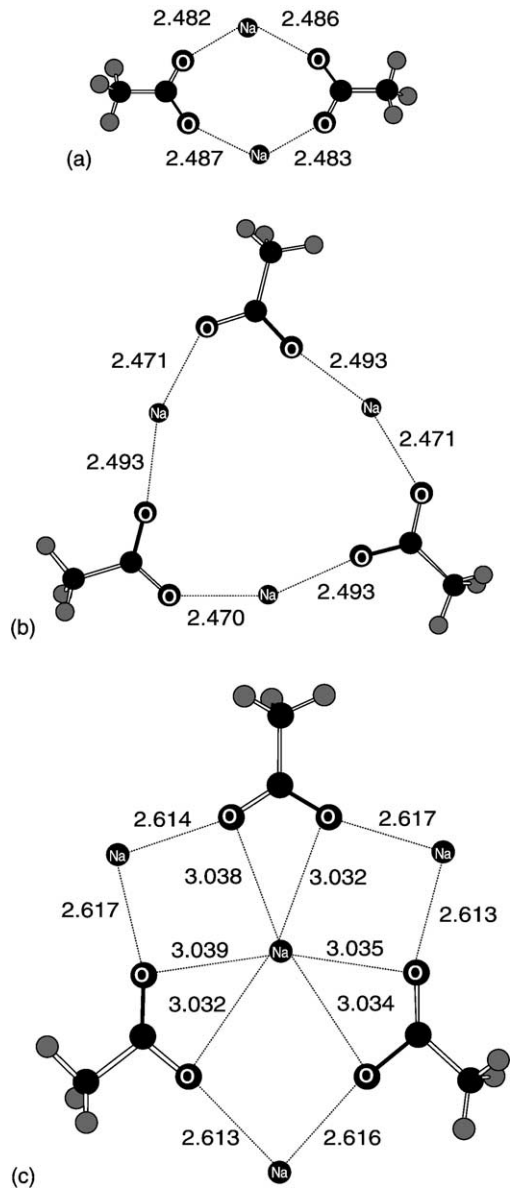

Fig. 10. PM3-optimized structures of (a) $(CH_3COONa)_2$; (b) $(CH_3COONa)_3$; and (c) $(CH_3COONa)_3Na^+$. Binding interactions are shown with dotted lines and the corresponding bond lengths are given in Å.

3.6. Calculated structures of cytosine clusters

Cytosine has two essentially isoenergetic tautomers, viz. a keto and an enol form [35–38].

Table 2
Heats of formation (ΔH_f) and binding energies of neutral clusters at the PM3 level of theory (kJ/mol at 298 K)

Species	Calculated ΔH_f	Binding energy of neutral cluster[a]
Neutral monomers		
CH_3COONa	−849	
Cytosine (keto)	−59	
Cytosine (enol)	−67	
Gly	−402	
Bet	−221	
H_2SO_4	−787	
Neutral clusters		
$(CH_3COONa)_2$	−1826	128
$(CH_3COONa)_3$	−2770	223
$(cytosine)_2$ (keto/keto)	−164	46
$(cytosine)_2$ (enol/enol)	−168	34
$(Gly)_2$	−840	37
$(Bet)_2$	−559	117
$(Arg)_2$[b]		189
Gly•••H_2SO_4	−1223	34
$GlyH^+$•••HSO_4^-[c]	−1148	−41
Bet•••H_2SO_4	−1083	75
$BetH^+$•••HSO_4^-	−1109	101
Ionic clusters		
$(CH_3COONa)_3Na^+$	−2823	
$(cytosine)_3H^+$ (all keto)	276	
$(Gly)_3H^+$	−648	
$(Bet)_3H^+$	−439	
Gly•••$GlyH^+$•••H_2SO_4	−1048	
$GlyH^+$•••HSO_4^-•••$GlyH^+$	−986	
Bet•••H_2SO_4•••$BetH^+$	−931	
$BetH^+$•••HSO_4^-•••$BetH^+$	−950	

[a] Energy needed for dissociation of the cluster to the monomers.
[b] Density functional theory value from Ref. [32].
[c] This zwitterion is 41 kJ/mol less stable than Gly + H_2SO_4.

The PM3-optimized structures of the keto/keto and enol/enol dimers are shown in Fig. 11. In either case, two intermolecular N–H•••O hydrogen bonds bring upon binding energies of 46 and 34 kJ/mol, respectively (Table 2). Thus, cytosine dimers are bound much more weakly than sodium acetate dimers. The most stable conformer of the proton-bound cytosine trimer found at the PM3 level has a linear structure and contains keto tautomers, with the central molecule being protonated and the two neutral units attached at opposite sides via N–H•••O hydrogen bonds (cf. Fig. 11). Sequential loss of cytosine monomers from this structure should be facile. In contrast, the loss of a $(cytosine)_2$ dimer necessitates rearrangement. We reason that this latter process is too slow to compete with the much simpler consecutive cleavages of cytosine monomers which, hence, is the only evaporation process observed experimentally upon CAD of $(cytosine)_3H^+$ (vide supra).

No calculations were performed for glycerol cluster ions, for which a multitude of isomeric structures exists. Experimentally, $(glycerol)_3H^+$ and $(cytosine)_3H^+$ were found to undergo only monomer evaporation (vide supra). In analogy to the proton-bound cytosine trimers, the evaporation reactivity of H^+-bound glycerol trimers is ascribed to (1) a low binding energy of neutral $(glycerol)_2$ and (2) the substantial reorientation necessary for the dissociating $(glycerol)_3H^+$ ions to lose an intact dimer in its most stable (and, hence, most strongly bound)

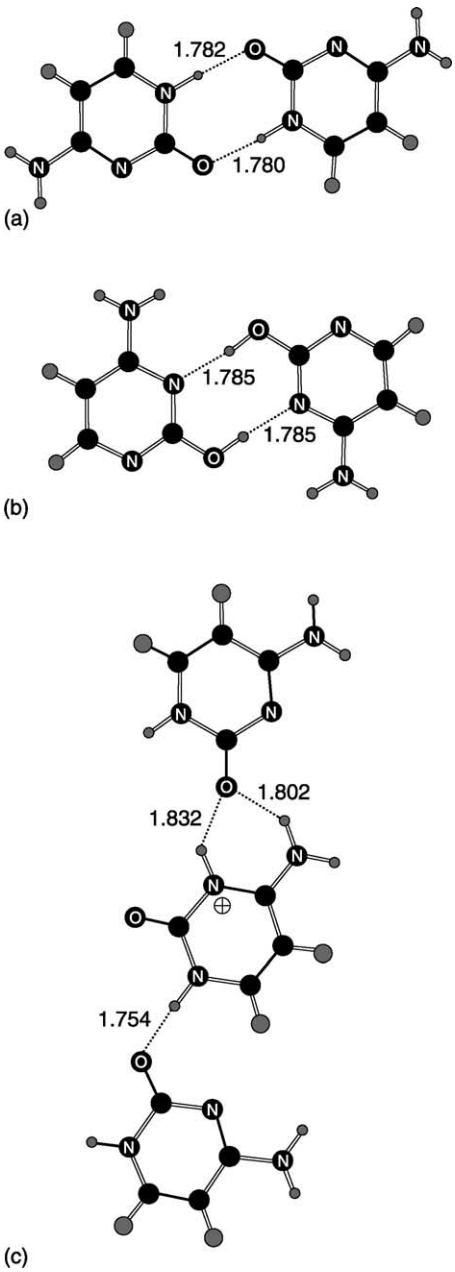

Fig. 11. PM3-optimized structures of (a, b) $(cytosine)_2$ dimers containing two (a) keto or (b) enol tautomers and (c) $(cytosine)_3H^+$ cluster ions containing keto tautomers. The lengths of intermolecular H-bonds are marked in Å.

configuration. These two reasons are also invoked to explain the lack of elimination of whole oligomers from the larger $(cytosine)_nH^+$ and $(glycerol)_nH^+$ clusters examined.

3.7. Calculated structures of glycine clusters

In the most stable structure of the $(Gly)_2$ dimer, the monomers are bound to each other through two O–H•••O hydrogen bonds between the carboxyl groups (Fig. 12). On the other hand, the $(Gly)_3H^+$ cluster ion has a distinct geometry, consisting of an N-protonated glycine that is charge-solvated intermolecularly by the other two glycine units via N–H•••N hydrogen bonds; the three COOH groups are far apart from each other (Fig. 12). The latter structure would impede the elimination of intact $(Gly)_2$ dimers, while readily permitting sequential Gly losses, as indeed observed in the experiment (see Section 3.4).

The proton-bound trimers of Asp, His, and Lys dissociate via sequential monomer eliminations, too. Also in these cluster ions, the monomer units are most likely arranged in geometries that differ significantly from those present in the respective neutral $(AA)_2$ dimers.

3.8. Calculated structures of betaine and arginine clusters

The dimer of betaine has the two monomers interacting head-to-tail (cf. Fig. 13). The positive charge of the quaternary ammonium sites is mainly distributed onto the H atoms of the methyl groups, as revealed by the corresponding Mulliken charges. This allows for strong attractive interactions between hydrogens in close proximity to the carboxylate groups and the O^- sites of the latter groups. In each Bet unit, one of the methyl H atoms is only 1.778 Å apart from a carboxylate oxygen. This distance is comparable to those found in hydrogen bonds (cf. Figs. 11–13). Additionally, the dimer is bound by the attractive forces in the two salt bridges formed at the termini of the monomers. The combined stabilizing interactions lead to a binding energy of 117 kJ/mol (Table 2), which is similar to that found in the ionically bound

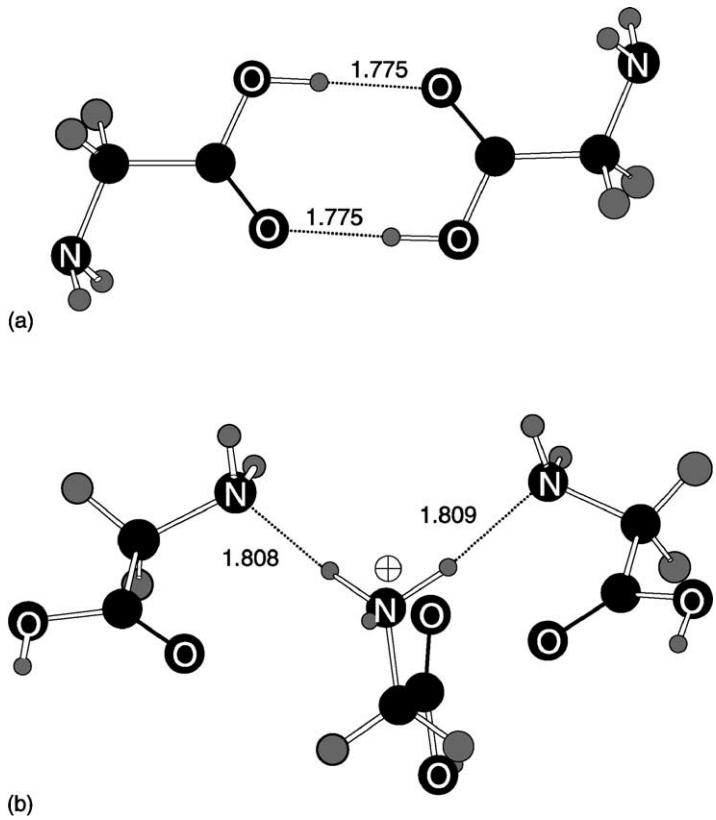

Fig. 12. PM3-optimized structures of (a) dimer $(Gly)_2$; and (b) cluster ion $(Gly)_3H^+$. The lengths of intermolecular H-bonds are marked in Å.

$(CH_3COONa)_2$ dimer and significantly higher than the binding energy of neutral hydrogen-bonded dimers, such as $(cytosine)_2$ and $(Gly)_2$ (Table 2).

The energy-minimized structure of $(Bet)_3H^+$ is included in Fig. 13. One Bet unit is protonated (at left), while the other two interact with each other and with the protonated monomer in a cyclical structure, involving salt bridges and H-bonds. Detachment of $BetH^+$ from $(Bet)_3H^+$ leaves two already interacting neutral units, which with some rotation can easily attain the most stable head-to-tail conformation of $(Bet)_2$. These structural and binding characteristics account for the observation of intact $(Bet)_2$ loss from collisionally excited $(Bet)_3H^+$ cluster ions.

Experimentally, $(Bet)_3H^+$ and $(Arg)_3H^+$ show parallel evaporation reactivities, both losing intact dimers upon CAD. Recent density functional theory calculations by Goddard and co-workers indicated that $(Arg)_2$ contains zwitterionic arginines arranged head-to-tail and held together by 189 kJ/mol via salt bridges and H-bonds [32]; this structure is completely analogous to the $(Bet)_2$ structure shown in Fig. 13. The guanidinium terminus of zwitterionic Arg can develop more H-bonds with an adjacent carboxylate group than the quaternary ammonium terminus of Bet; this and the closer proximity of the ion pairs in $(Arg)_2$ vs. $(Bet)_2$ provide a rationale for the larger binding energy of the former dimer (Table 2).

There are no computational data about $(Arg)_3H^+$. The neutral trimer, $(Arg)_3$, is predicted by Goddard and co-workers to contain a cyclic array of salt bridges [32]. Most likely, $(Arg)_3H^+$ has a similar structure, with binding interactions between the neutral Arg units, so that an intact $(Arg)_2$ dimer can be eliminated.

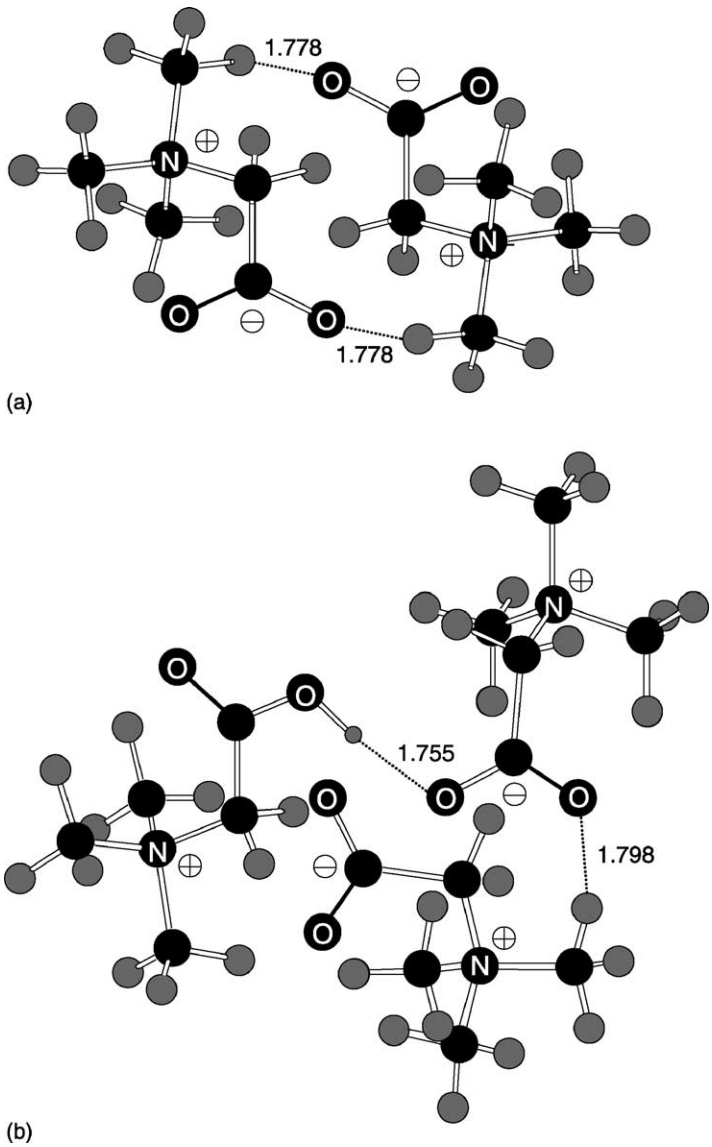

Fig. 13. PM3-optimized structures of (a) dimer $(Bet)_2$; and (b) cluster ion $(Bet)_3H^+$. The lengths of intermolecular H-bonds are marked in Å.

3.9. Calculated structures of mixed amino acid–sulfuric acid clusters

All $H_2SO_4(AA)_2H^+$ cluster ions investigated (AA = Asp, His, Lys, Bet, Arg) eliminate whole H_2SO_4 •••AA heterodimers upon CAD (see Section 3.3). The Gly system was not probed experimentally, because the corresponding cluster ion is not formed with sufficient intensity to give a useable N_fR spectrum. We, however, employed the H_2SO_4•••Gly and $H_2SO_4(Gly)_2H^+$ clusters as models of non-zwitterionic complexes in the semiempirical calculations, as the larger systems proved to be computationally intractable.

The lowest-energy structure of the H_2SO_4/Gly cluster contains the neutral forms of these molecules

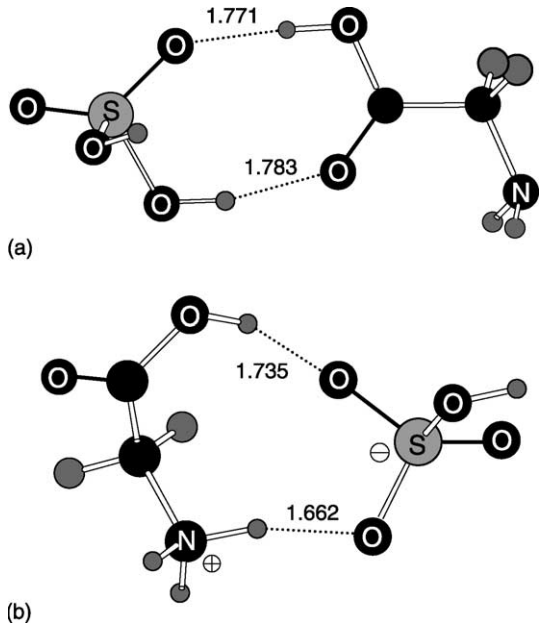

Fig. 14. PM3-optimized structures of (a) the hydrogen-bonded Gly•••H_2SO_4 complex; and (b) the $GlyH^+$•••HSO_4^- ion pair. The lengths of hydrogen bonds are given in Å.

connected through two O–H•••O hydrogen bonds between the H_2SO_4 unit and the carboxyl group of glycine (Fig. 14a). This structure is strikingly similar to that of the $(Gly)_2$ dimer (cf. Fig. 12a), which is reflected by the corresponding very similar binding energies of 34 and 37 kJ/mol, respectively. The $GlyH^+$•••HSO_4^- ion pair (Fig. 14b) lies 75 kJ/mol above the nonionic complex and is not bound relative to H_2SO_4 + Gly (Table 2).

The most stable isomer of the $H_2SO_4(Gly)_2H^+$ cluster ion at the PM3 level is the cyclic, charge-solvated species depicted in Fig. 15a; this cluster ion can be viewed as a N^+–H•••N proton-bound dimer of Gly, with the two Gly monomers bridged by the H_2SO_4 molecule via N^+–H•••O and O–H•••O hydrogen bonds. In the most stable ion–zwitterion configuration $GlyH^+$•••HSO_4^-•••$GlyH^+$, the + − + charges are arranged linearly to maximize attractive and minimize repulsive forces (Fig. 15b). Even though this structure is stabilized by additional O–H•••O H-bonds, it is signif-

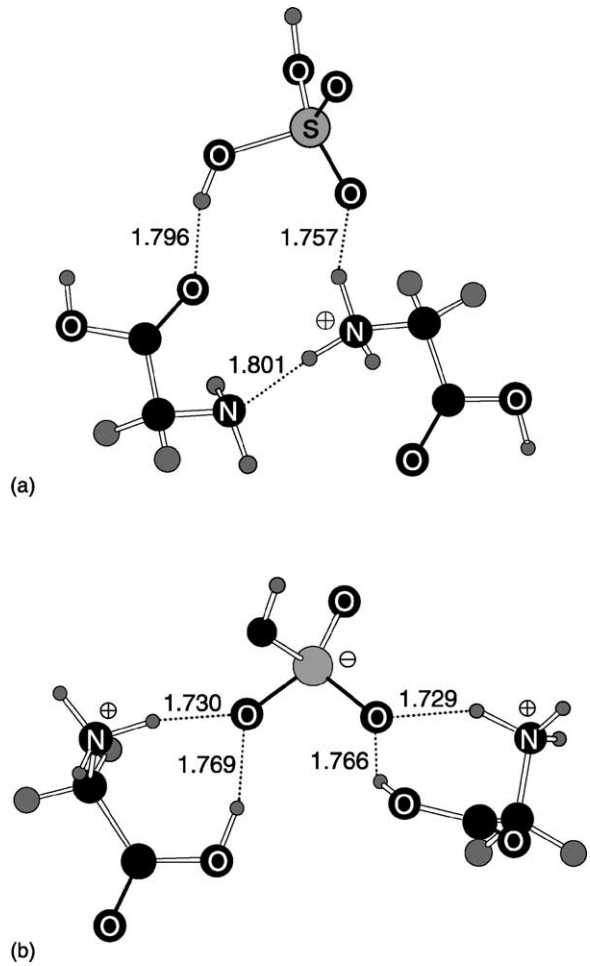

Fig. 15. PM3-optimized structures of $H_2SO_4(Gly)_2H^+$ cluster ions: (a) charge solvated isomer; and (b) salt-bridged isomer. The lengths of hydrogen bonds are given in Å.

icantly less stable than the charge-solvated complex (Table 2).

Unlike the $(Gly)_3H^+$ geometry, where the outer, uncharged monomers do not interact with each other (Fig. 12b), the uncharged cluster constituents of $H_2SO_4(Gly)_2H^+$ have bonding interactions both with the charge site as well as with one another (Fig. 15a). The latter feature facilitates the elimination of intact H_2SO_4•••Gly clusters from $H_2SO_4(Gly)_2H^+$. All $H_2SO_4(AA)_2H^+$ precursor ions studied lose H_2SO_4 but not AA, suggesting that bonds to H_2SO_4 are

loosened first upon collisional activation. Cleavage of the N^+–H•••O hydrogen bond in $H_2SO_4(Gly)_2H^+$ (cf. Fig. 15a) leaves the detaching H_2SO_4 moiety still bound to the neutral Gly molecule via a O–H•••O hydrogen bond. H_2SO_4 may detach completely or rotate to form a second O–H•••O hydrogen bond to the neutral Gly unit, thereby enabling the loss of a complete H_2SO_4•••Gly cluster.

The computational data on $(Gly)_2$ and $(Gly)_3H^+$ vis-a-vis H_2SO_4•••Gly and $H_2SO_4(Gly)_2H^+$ reveal that the precursor ion structure plays a critical role in the ensuing evaporation mechanism. Note that the binding energies of Gly•••Gly and H_2SO_4•••Gly clusters are practically identical (Table 2) but that only the latter is eliminated in one piece, because its components already interact in the precursor ion.

The evaporation behavior of $H_2SO_4(AA)_2H^+$ cluster ions with AA = Asp, His, and Lys is readily rationalized by cyclic structures analogous to that predicted for the Gly analog. The basic site protonated and participating in hydrogen bonds presumably is the N-terminal NH_2 group in Asp (as in Gly) but the side chain substituents in His and Lys clusters [22]. In either case, the unique characteristic leading to intact H_2SO_4•••AA heterodimer loss should be the existence of intermolecular interactions between the H_2SO_4 and AA units in the $H_2SO_4(AA)_2H^+$ precursor ions.

The clusters of betaine, a naturally zwitterionic amino acid were calculated separately. In its most stable geometry, the charge-solvated complex between H_2SO_4 and the betaine zwitterion, i.e., H_2SO_4•••$^+$Bet$^-$ (also designated as H_2SO_4•••Bet), contains two hydrogen bonds, connecting the carboxylate group to a S–OH group and one of the CH_3 protons to a S=O group (Fig. 16a). As mentioned previously (Section 3.8), the quaternary ammonium charge is mainly distributed onto the methyl hydrogens, which allows them to form hydrogen bonds with nearby negatively charged centers. The binding energy of the described heterodimer is 75 kJ/mol (Table 2). A dimer of substantially lower energy is generated by intermolecular proton transfer from H_2SO_4 to Bet. In the resulting $BetH^+$•••HSO_4^- ion pair (Fig. 16b), three hydrogen bonds can evolve, leading to a binding energy of 101 kJ/mol (Table 2).

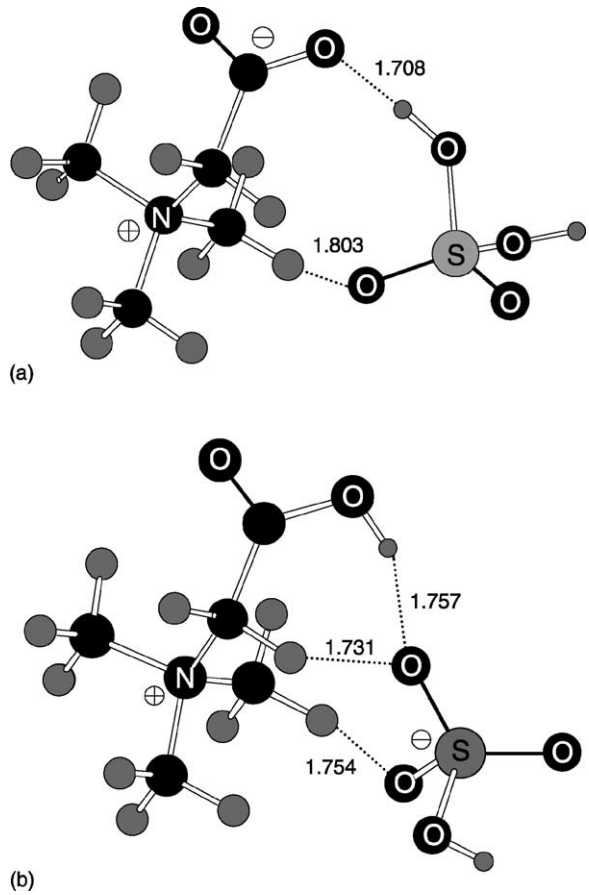

Fig. 16. PM3-optimized structures of (a) Bet•••H_2SO_4; and (b) $BetH^+$•••HSO_4^- clusters. The lengths of hydrogen bonds are given in Å.

The most stable isomer of $H_2SO_4(Bet)_2H^+$ arises by combining two protonated betaine units with deprotonated sulfuric acid, $BetH^+$•••HSO_4^-•••$BetH^+$, which is illustrated in Fig. 17b. This structure is 19 kJ/mol lower in energy than the alternative combination Bet•••H_2SO_4•••$BetH^+$ (Fig. 17a). The higher stability of the salt-bridged isomer is attributed to the larger separation of the methyl groups of its Bet units, which reduces repelling forces. An important aspect is the similarity of

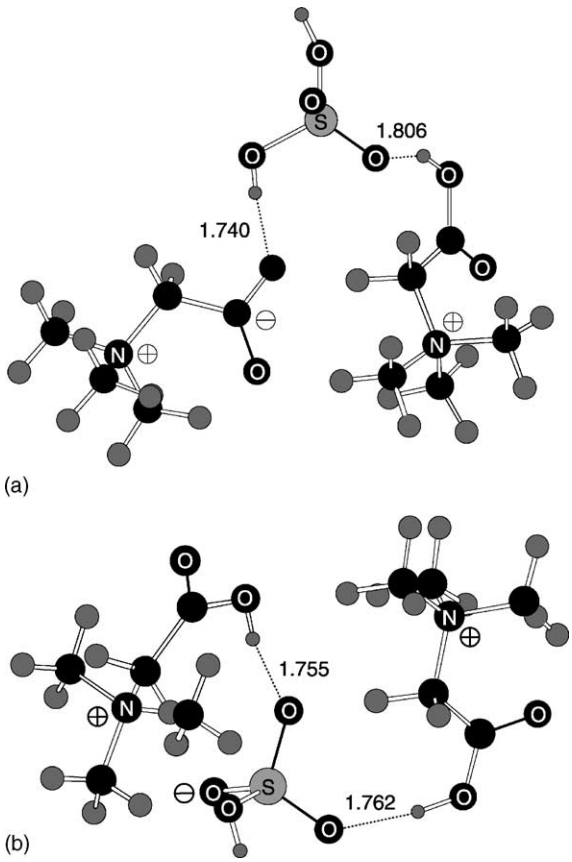

Fig. 17. PM3-optimized structures of $H_2SO_4(Bet)_2H^+$ cluster ions: (a) charge solvated isomer Bet•••H_2SO_4•••$BetH^+$; and (b) salt-bridged isomer $BetH^+$•••HSO_4^-•••$BetH^+$. The lengths of hydrogen bonds are given in Å.

bonding interactions in the $BetH^+$•••HSO_4^- ion pair (Fig. 16b) and the $BetH^+$•••HSO_4^- portion of the $BetH^+$•••HSO_4^-•••$BetH^+$ cluster ion (Fig. 17b). Based on these structural features, the elimination of intact $BetH^+$•••HSO_4^- clusters from $BetH^+$•••HSO_4^-•••$BetH^+$ is a kinetically favorable process and releases a particularly stable cluster. The convolution of these factors explains the high yield of Bet/H_2SO_4 cluster loss from $H_2SO_4(Bet)_2H^+$, which was attested by the much higher relative abundance of $BetH^+$ in the corresponding N_fR spectrum (Fig. 8b) as compared to the AAH^+ abundances in the N_fR spectra of the Asp, His or Lys systems (Figs. 6, 7a and b). On the other hand, the N_fR characteristics of $H_2SO_4(Arg)_2H^+$ and $H_2SO_4(Bet)_2H^+$ are quite similar (cf. AAH^+ abundances in Fig. 8 vs. Figs. 6–7). We therefore conclude that Bet and Arg form structurally comparable H_2SO_4•••AA clusters and $H_2SO_4(AA)_2H^+$ cluster ions, the most stable structures of the Arg complexes being the $ArgH^+$•••HSO_4^- ion pair and the $ArgH^+$•••HSO_4^-•••$ArgH^+$ double salt bridge, respectively. In fact, the tendency to abstract a proton from H_2SO_4 in order to generate ion pairs (salt bridges) should be more pronounced for Arg than Bet owing to the higher proton affinity of the former molecule (Table 1).

4. Conclusions

N_fR spectra provide conclusive information on whether intact neutral clusters are evaporated from dissociating larger cluster ions. Semiempirical calculations about the structures of the evaporated clusters and their precursor ions and about the binding energetics of the neutral clusters reveal that the major requirement for the liberation of complete clusters vis-a-vis sequential monomer loss is a suitable structure of the precursor cluster ion. Precursor ions with interactions between the components to be eliminated as a neutral cluster do release such clusters upon CAD. In contrast, if these components are not near each other to interact, they are cleaved consecutively. Cluster ions with cyclic or ring-like structures, in which multiple binding interactions can develop among the cluster ion constituents, generally undergo intact dimer (or larger oligomer) evaporation.

The neutral clusters evaporated from dissociating cluster ions are bound through electrostatic interactions. In the cases studied, these interactions involve hydrogen bonds and/or ion pairs (salt bridges). Whenever the most stable form of an overall neutral cluster contains salt bridge(s), the binding energy is particularly high (cf. Table 2). A high binding energy in the neutral cluster increases the yield of its evaporation as an intact unit.

Acknowledgements

Financial support from the National Science Foundation (grants CHE-9725003 and 0111128) is gratefully acknowledged.

References

[1] C.Y. Ng, T. Baer, I. Powis (Eds.), Cluster Ions, Wiley, Chichester, 1993.
[2] A.W. Castleman Jr., R.G. Keesee, Science 241 (1988) 36.
[3] A.W. Castleman Jr., K.W. Bowen Jr., J. Phys. Chem. 100 (1996) 12911.
[4] C. Lifshitz, in: C.Y. Ng, T. Baer, I. Powis (Eds.), Cluster Ions, Wiley, Chichester, 1993, p. 121.
[5] W.Y. Feng, C. Lifshitz, J. Phys. Chem. 98 (1994) 6075.
[6] C. Lifshitz, W.Y. Feng, Int. J. Mass Spectrom. Ion Process. 146/147 (1995) 223.
[7] H.J. Hwang, D.K. Sensharma, M.A. El-Sayed, Chem. Phys. Lett. 160 (1989) 243.
[8] M.A. El-Sayed, J. Phys. Chem. 95 (1991) 3898.
[9] M.J. Polce, S. Beranova, M.J. Nold, C. Wesdemiotis, J. Mass Spectrom. 31 (1996) 1073.
[10] M.J. Polce, M.M. Cordero, C. Wesdemiotis, P.A. Bott, Int. J. Mass Spectrom. Ion Process. 113 (1992) 35.
[11] P.C. Burgers, J.L. Holmes, A.A. Mommers, J.K. Terlouw, Chem. Phys. Lett. 102 (1983) 1.
[12] P.C. Burgers, J.L. Holmes, A.A. Mommers, J.E. Szulejko, J.K. Terlouw, Org. Mass Spectrom. 19 (1984) 442.
[13] R. Clair, J.L. Holmes, A.A. Mommers, P.C. Burgers, Org. Mass Spectrom. 20 (1985) 207.
[14] J.L. Holmes, A.A. Mommers, J.K. Terlouw, C.E.C.A. Hop, Int. J. Mass Spectrom. Ion Process. 68 (1986) 249.
[15] M.J. Polce, C. Wesdemiotis, Rapid Commun. Mass Spectrom. 10 (1996) 235.
[16] (a) U. Burkert, N.L. Allinger, Molecular Mechanics, ACS, Washington, DC, 1982;
(b) J.A. McCammon, S. Harvey, Dynamics of Proteins and Nucleic Acids, Cambridge University Press, Cambridge, UK, 1987.
[17] CambridgeSoft Corporation, Cambridge, MA.
[18] J.J.P. Stewart, J. Comput. Chem. 10 (1989) 209 and 221.
[19] S. Beranova, C. Wesdemiotis, J. Am. Soc. Mass Spectrom. 5 (1994) 1093.
[20] F.W. McLafferty, F. Turecek, Interpretation of Mass Spectra, 4th ed., University Science Books, Mill Valley, 1993.
[21] S.G. Lias, J.E. Bartmess, J.F. Liebman, J.L. Holmes, R.D. Levin, W.G. Mallard, J. Phys. Chem. Ref. Data 17 (Suppl. 1) (1988).
[22] (a) E.P.L. Hunter, S.G. Lias, J. Phys. Chem. Ref. Data 27 (1998) 413;
(b) http://webbook.nist.gov/chemistry
[23] J.M. Rice, G.O. Dudek, M. Barber, J. Am. Chem. Soc. 87 (1965) 4569.
[24] R. Importa, G. Scalmani, V. Barone, Int. J. Mass Spectrom. 201 (2000) 321.
[25] M. Dey, F. Moritz, J. Grotemeyer, E.W. Schlag, J. Am. Chem. Soc. 116 (1994) 9211.
[26] M.M. Cordero, C. Wesdemiotis, Org. Mass Spectrom. 28 (1993) 1041.
[27] S. Campbell, M.T. Rodgers, E.M. Marzluff, J.L. Beauchamp, J. Am. Chem. Soc. 117 (1995) 12840.
[28] P.D. Schnier, W.D. Price, R.A. Jockusch, E.R. Williams, J. Am. Chem. Soc. 118 (1996) 7178.
[29] R.A.J. O'Hair, J.H. Bowie, S. Gronert, Int. J. Mass Spectrom. Ion Process. 117 (1992) 23.
[30] J.S. Patrick, S.S. Yang, R.G. Cooks, J. Am. Chem. Soc. 118 (1996) 231.
[31] A. Melo, M.J. Ramos, W.B. Floriano, J.A.N.F. Gomes, J.F.R. Leao, A.L. Magaehaes, B. Maigret, M.C. Nascimento, N. Reuter, J. Mol. Struct. (Theochem.) 463 (1999) 81.
[32] R.R. Julian, J.L. Beauchamp, W.A. Goddard, J. Phys. Chem. A 106 (2002) 32.
[33] E.F. Strittmatter, E.R. Williams, J. Phys. Chem. A 104 (2000) 6069.
[34] R.R. Julian, R. Hodyss, J.L. Beauchamp, J. Am. Chem. Soc. 123 (2001) 3577.
[35] P.U. Civcir, J. Mol. Struct. (Theochem.) 532 (2000) 157.
[36] R. Kobayashi, J. Phys. Chem. A 102 (1998) 10813.
[37] L. Gorb, Y. Podolyan, J. Leszczynski, J. Mol. Struct. (Theochem.) 487 (1999) 47.
[38] J.R. Sambrano, A.R. deSouza, J.J. Queralt, J. Andres, J. Chem. Phys. Lett. 317 (2000) 437.